Available online at www.sciencedirect.com

ScienceDirect

International Journal of Mass Spectrometry 255–256 (2006) 213–224

International Journal of Mass Spectrometry

www.elsevier.com/locate/ijms

Getting a theoretical handle on fullerene ions: Quantum chemical calculations on the reactions of $C_{60}{}^{+}$, $C_{60}{}^{2+}$ and $C_{60}{}^{3+}$ with ammonia[☆]

Simon Petrie[*]

Department of Chemistry, The Faculties, Australian National University, Canberra, ACT 0200, Australia

Received 30 November 2005; received in revised form 9 January 2006; accepted 10 January 2006
Available online 17 February 2006

Abstract

Hybrid density functional theory calculations at the B3-LYP/6-31G** level of theory are used to explore the interactions between singly, doubly, and triply charged fullerene cations and ammonia. The calculations illuminate (and generally support) several aspects of the previously-reported experimental results for these systems. Primary adduct formation is exothermic but is hindered by an energetically costly localized distortion of the fullerene cage at the site of addition, as the 'chosen' carbon atom shifts from strained sp^2 to sp^3 coordination. The 50–75 kJ mol^{-1} 'deformation energy' is substantially larger than the residual strength of the bond between $C_{60}{}^{+}$ and NH_3. Although the deformation energy rises with increasing fullerene ion charge state, it does so less steeply than does the electrostatic attraction between $C_{60}{}^{n+}$ and NH_3, so that the overall bond strength to NH_3 is progressively and substantially larger for the di- and tricationic adduct ions. For all charge states, a proton-bound structure is found to be the energetically preferred secondary adduct, but for dicationic and tricationic adducts formation of a secondary adduct is significantly less exothermic than proton transfer. It appears that the failure of $C_{60}{}^{+}$ to add measurably to nucleophiles weaker than NH_3 arises because such nucleophiles are not able to overcome the required deformation energy to effect bond formation. We find also that, in contrast to a simple electrostatically-driven model of 'handle' formation (in which it was proposed that the most strongly bound doubly-derivatized fullerene dications would be those for which the 'handles' were most widely separated across the fullerene framework) the lowest-energy double-handled adducts are in fact those for which the remaining resonance stabilization is greatest, with electrostatic considerations apparently taking a back seat on the question of relative stability. Similar considerations appear to apply to the double-handled tricationic adducts.

Keywords: Association reaction; C60; Hybrid density functional theory; Molecular polycation; Quantum chemical calculation; Proton transfer

1. Introduction

Buckminsterfullerene, C_{60}, the most well-rounded allotrope of carbon, has been subjected to an almost uncountable number of chemical inquisitions [1–8] since its discovery around 2 decades ago [9,10]. Various research groups have seen fit to strip it of an improbable number of electrons [11,12], to couple it with various inappropriate chemical partners [13,14], to stuff it with sundry unreasonable atoms and molecules [15–17], and to pummel it at frighteningly high velocities against a range of unrelenting surfaces [18]. In this context, the treatment that C_{60} has received at the hands of the Bohme group [19–22] can be seen to be comparatively benign. Using the selected-ion flow tube technique, Bohme and co-workers have systematically assessed the reactivity of fullerene ions, most frequently $C_{60}{}^{+}$, $C_{60}{}^{2+}$, and $C_{60}{}^{3+}$, with a broad range of gas-phase neutrals. Two somewhat surprising tendencies soon emerged from these studies. First, the multiply-charged fullerenes such as $C_{60}{}^{2+}$ and $C_{60}{}^{3+}$ were often distinctly less prone to exhibit single-charge transfer to reactant neutrals than was expected on the basis of a simple comparison of ionization energies [23–26]. For example, based on $IE(C_{60}{}^{+}) = 11.39 \pm 0.05$ eV [27] and $IE(C_2H_4) = 10.507$ eV, the reaction

$$C_{60}{}^{2+} + C_2H_4 \rightarrow C_{60}{}^{+} + C_2H_4{}^{+} \quad (1)$$

is almost one eV exothermic, and yet this product channel was not detected at all, in competition only with a highly inefficient association process [24]. The second surprise was that highly inefficient association (or, so far as it could be established, no association whatsoever) was, it transpired, something

---

[☆] To Diethard, friend and mentor.

[*] Tel.: +61 2 6125 7931; fax: +61 2 6125 0760.
E-mail address: simon.petrie@anu.edu.au.

1387-3806/$ – see front matter © 2006 Elsevier B.V. All rights reserved.
doi:10.1016/j.ijms.2006.01.026

which fullerene ions did extremely well. It began to seem that C_{60}^+, in particular, did nothing else. This author recalls that, during our first few days of assaying the reactivity of C_{60}^+, we had tested virtually the complete Bohme collection of lecture-bottles and volatile samples, running through H_2, N_2, NO, N_2O, CO, CO_2, OCS, CS_2, CH_4, C_2H_2, C_2H_4, C_2H_6, CH_3CCH, H_2O, H_2CO, CH_3OH, CH_3OCH_3, HCOOH, $HCOOCH_3$, CH_3CHO, CH_3COCH_3, *c*-C_2H_4O, HCN, and CH_3CN, without obtaining the slightest indication of a reaction of C_{60}^+ with any of these species. Ammonia and the amines we had left towards the end, because they were malodorous and would take longer to pump out of the vacuum system after their introduction. It transpired, however, that C_{60}^+ had a soft spot for amines, and would associate with them [28]. Under our reactive conditions of $T \sim 300$ K and $P \sim 0.35$ Torr (helium buffer gas pressure), we obtained effective bimolecular association rate coefficients of less than 1×10^{-12} cm^3 molecule^{-1} s^{-1} for the reaction:

$$C_{60}^+ + NH_3(+M) \rightarrow C_{60}NH_3^+(+M^*) \quad (2)$$

ranging up to near-collision-rate values for the analogous association reactions with di- and trimethylamine [28]. Furthermore, although the primary association reactions with methylamine and with ethylamine were comparatively slow ($k = 1.5 \times 10^{-11}$ and 5.0×10^{-11} cm^3 molecule^{-1} s^{-1}, respectively), a subsequent secondary addition of another amine was found to be efficient in these systems, as was also observed for dimethylamine (but *not* for trimethylamine). The observed reactivity of C_{60}^{2+} and C_{60}^{3+} with ammonia and the amines was, fittingly, more ‘highly charged’: reactions invariably occurred at close to the collision rate, with addition often competing with charge transfer (and, from the multiply-charged adducts, proton transfer) [28–30].

The present work revisits the reactivity of fullerene ions with amines, this time from the fresh standpoint of computational chemistry, with the hope of rationalizing aspects of the fullerene ion/amine reaction mechanism. For the sake of computational expediency, ammonia is the only ligand surveyed here: its reactivity with C_{60}^+, C_{60}^{2+}, and C_{60}^{3+} is explored in the context of association and proton transfer processes.

2. Theoretical methods

The present work uses hybrid density functional theory calculations, namely the combination of Becke’s three-parameter exchange functional [31] with the correlation functional of Lee, Yang, and Parr [32] (B3-LYP), to characterize stationary points on various potential energy surfaces appropriate to the interaction of fullerene ions with ammonia. In concession to the large size of the species involved, results are reported using a comparatively modest basis set, 6-31G**. Calculations were pursued with the imposition of at least C_s symmetry. Nonetheless, despite the use of a small basis set and the recourse to symmetric structures, it did not prove possible to obtain fundamental vibrational frequencies or zero-point energy (ZPE) corrections for the species concerned. A further limitation of the computational method is that basis set superposition error (BSSE) [33] was not addressed. With these limitations in mind, it is anticipated that the computed bond strengths and other relative energies are unlikely to be highly accurate: neglect of both ZPE and BSSE is likely to result in some exaggeration of adduct ion bond strengths.

All calculations were performed using the GAUSSIAN98 program suite [34].

3. Results and discussion

3.1. Reaction of NH_3 with C_{60}^+

The energetic and structural data obtained for the interactions of C_{60}^+ with one or two NH_3 molecules are summarized in Table 1, while depictions of the optimized geometries are shown in Fig. 1. All calculations were pursued only on the doublet electronic state surface, since the reactant ion C_{60}^+ has one unpaired electron: spin contamination was found to be minor in all calculations, with expectation values $\langle s^2 \rangle$ consistently below 0.78 (which compares with the value of 0.75 expected for a pure doublet).

Of the parameters detailed in Table 1, some require further explanation. The angle $\theta(NCC_\alpha)$ is defined as the mean of the three values for the angle between *N*, the *ipso* carbon, and an α carbon. This value provides a measure of the pyramidalization

Table 1
Energetic and structural details obtained, at the B3-LYP/6-31G** level of theory, for species relevant to the reactions of C_{60}^+ and secondary ions with ammonia

Species	$E_e(C_{60}X^{n+})$[a] (hartree)	E_{rel}[b] (kJ mol^{-1})	r(C–N) (Å)	$\theta(NCC_\alpha)$[c] (°)	$q_{Mull}(N)$[d]	E_{deform}[e] (kJ mol^{-1})	Other parameters
$C_{60}^+ + 2NH_3$	−2285.910695	0.0	–	101.5	–		
$(C_{60}\cdot NH_3)^+$ ($^2A'$) + NH_3	−2342.4777205	−24.3	1.616	108.9	+0.52	52.5	
$(C_{60}\cdot NH_3\cdot NH_3)^+$ ($^2A'$)	−2399.0725034	−121.5	1.558	110.0	+0.49(α); +0.13(β)		$r(N_\alpha–H) = 1.095$; $r(H–N_\beta) = 1.670$
$(H_3N\cdot C_{60}\cdot NH_3)^{2+}$ ($^2A''$)	−2399.0436002	−45.6	2.862	101.8	+0.07 × 2		
$C_{60}NH_2 + NH_4^+$	−2342.0985531	+57.3			−0.06		

[a] Total energy for the identified fullerene-containing species, excluding zero-point vibrational energy.

[b] Energy of the indicated combination of species (at 0 K), expressed relative to the total energy of the three reactants $C_{60}^+ + 2NH_3$.

[c] Pyramidalization angle of the anchorage carbon atom(s), defined as detailed in the text.

[d] Calculated Mulliken charge on the nitrogen atom(s), with contributions from H atoms incorporated into N.

[e] Energy of deformation of the anchorage carbon atom, defined as detailed in the text.

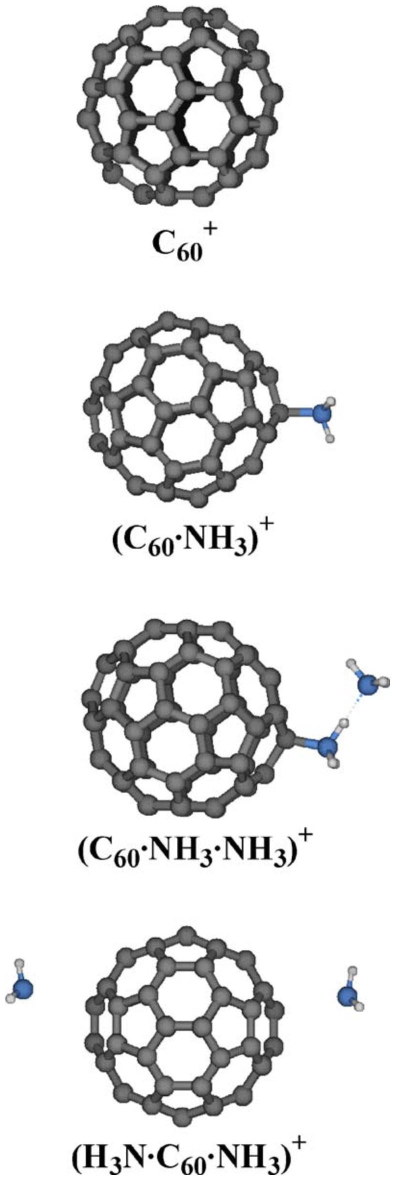

Fig. 1. Structures relevant to the reactions of $C_{60}{}^+$ with ammonia, optimized at the B3-LYP/6-31G** level of theory.

at the *ipso* C. For the bare fullerene ion $C_{60}{}^+$, this angle is also defined (with the place of N here being taken by the local body diagonal). The atomic charge $q_{\mathrm{Mull}}(N)$ is the Mulliken charge on the associated N atom (with charges on hydrogen incorporated into this N value). For adducts involving the direct attachment of the first or second NH_3 to the fullerene cage, the 'deformation energy' E_{deform} is defined as the difference in energy between the bare fullerene ion (or, for addition of a second NH_3, the primary adduct ion) in its optimized geometry and in its distorted form within the appropriate adduct ion. Where relevant, the distance of bridging protons between nitrogen atoms is also provided. Finally, it should be noted that in all cases the energetic and structural details in the table are for geometries in which the appended NH_3 moieties have staggered conformations with respect to the local fullerene network. Calculations on the corresponding eclipsed conformations were also pursued but were invariably found to be higher in energy than the staggered arrangements.

It can be seen from the table that the reaction between $C_{60}{}^+$ and NH_3 produces an adduct ion, $(C_{60}{\cdot}NH_3)^+$ ($^2A'$), with an unusually long (1.62 Å) and very weak C–N bond. The very low value for this bond strength, of 24 kJ mol^{-1}, is, if anything, expected to be an overestimate due to the neglect of both zero-point vibrational energy and basis set superposition error; but both of these neglected effects are likely to be minor given the weakness of the interaction and the large C–N separation. The very low strength of the bond produced through association is fully consistent with the experimental observation [28] that the association reaction is very slow ($k_{\mathrm{eff}} < 1 \times 10^{-12}$ cm^3 molecule^{-1} s^{-1} at 300 K and 0.35 Torr).

The bare fullerene ion has a 'pyramidalization angle' $\theta(\mathrm{NCC}_\alpha)$ of 101.5°, which is intermediate between the corresponding values for unstrained sp^2 hybridization (90°) and pure sp^3 hybridization (109.5°). The very weak adduct ion $(C_{60}{\cdot}NH_3)^+$ has a value ($\theta(\mathrm{NCC}_\alpha) = 108.9°$) which is almost perfectly tetrahedral. This is, in some respects, surprising. The calculated Mulliken charge on NH_3 is only about half a full positive charge, suggesting that the adduct ion has about equal proportions of character resulting from the ammonia adduct $C_{60}{}^+{\cdot}NH_3$ and from the ammonium-like ion $C_{60}NH_3{}^+$ (although it should also be noted that the Mulliken charge distribution often has a tendency to underestimate the magnitude of charge localization on individual atoms). The electrostatic complex $C_{60}{}^+{\cdot}NH_3$ would be expected to carry negligible charge on NH_3 and minor distortion of the fullerene ion's surface, which appears inconsistent with the degree of puckering that is evident from the adduct's $\theta(\mathrm{NCC}_\alpha)$ value. However, it is clear that the deformation in the fullerene ion's structure, arising from NH_3 addition, is not without cost. Calculations on the 'relaxed' $C_{60}{}^+$ geometry, and on $C_{60}{}^+$ with the geometry of the fullerene fragment within the optimized $(C_{60}{\cdot}NH_3)^+$ structure, indicate that the 'deformation energy' for the fullerene ion is 52.5 kJ mol^{-1}. This is a measure of the fullerene ion's resistance to derivatization, and rationalizes the very low bond strength seen in the $(C_{60}{\cdot}NH_3)^+$ adduct. Without the need for reshaping of the carbon framework around the site of addition, the C–N bond formed would have an expected intrinsic strength of almost 80 kJ mol^{-1}, based on the difference between E_{distort} and E_{rel}.

It is worth comparing the result for $C_{60}{}^+{\cdot}NH_3$ adduct formation with a simple model, namely adduct formation between $C_2H_4{}^+$ (i.e., the simplest alkene radical ion) and NH_3. At the B3-LYP/6-31G** level of theory, and neglecting zero-point vibrational energy, the $C_2H_4{}^+{\cdot}NH_3$ adduct possesses a bond strength of 257.0 kJ mol^{-1}, a C–N bond length of 1.564 Å, and a $\theta(\mathrm{NCC}_\alpha)$ value of 106.8°. This may be compared further with calculations performed using the generally authoritative CBS-APNO method [35], which yield broadly similar structural data ($r(\mathrm{C–N}) = 1.541$ Å, $\theta(\mathrm{NCC}_\alpha) = 111.1°$) and a bond strength of 239.8 kJ mol^{-1}. While it is reasonable to expect that the intrinsic strength of the $C_2H_4{}^+/NH_3$ interaction exceeds that for $C_{60}{}^+/NH_3$ due to the heightened importance of charge stabilization by ammonia addition in the smaller system (C_2H_4 has a significantly higher ionization energy than NH_3, 10.507 eV versus 10.070 eV), the order-of-magnitude difference between the $C_2H_4^+$–NH_3 and C_{60}^+–NH_3 bond strengths demonstrates very clearly the fragility of the latter bond. Since the calculated geometric parameters for the two complexes do not differ greatly, the disparity in bond strengths further supports the assertion that the fullerene/ligand bond is significantly weakened due to the need for distortion of the fullerene cage.

We have also attempted to locate adduct ion structures for the species $(C_{60}{\cdot}NCH)^+$ and $(C_{60}{\cdot}OH_2)^+$. These species, resulting from reaction of C_{60}^+ with HCN and H_2O, respectively, do not appear to form bound stationary points. This observation is qualitatively consistent with the observation that C_{60}^+ is not ostensibly reactive with either HCN or H_2O in experimental studies [36,37], and suggests that the low reactivity of C_{60}^+ is connected to the requirement for fullerene surface deformation (as measured, for example, by the change in $\theta(NCC_\alpha)$ value from the bare fullerene ion to the adduct) as the anchorage carbon's hybridization changes from strained sp^2 to sp^3. It appears that such deformation is only energetically feasible when the coordinating base is of sufficient strength. The proton affinity (PA) of the reactant neutral, which measures the strength of proton attachment to a base, may also be a relevant predictor of the strength of C_{60}^+ attachment: it is notable that all of the species with which C_{60}^+ is experimentally found not to react have PA values below that of NH_3, while the amines to which C_{60}^+ adds more rapidly all have a PA above that of NH_3. Consistent also with an energetic resistance of C_{60}^+ to pyramidalization at the point of ligand attachment is the observation that smaller fullerene ions such as C_{56}^+ and C_{58}^+, which have some quite highly pyramidalized C atoms by virtue of their 'adjacent pentagon' fullerene lattice, display a much greater propensity to undergo addition than does C_{60}^+ itself [38]. In essence, the deformation energy for an adjacent-pentagon fullerene is a much smaller quantity than for C_{60}^+ itself, allowing the formation of more strongly bound adducts to C_{56}^+, C_{58}^+, and similar adjacent-pentagon fullerenes [38].

Can C_{60}^+ add a second ammonia molecule? Our calculations suggest that it can, despite the lack of evidence for a second addition in the experimental studies of the $C_{60}^+ + NH_3$ reaction [28]. The experimental limitation is that the observed signal strength for $(C_{60}{\cdot}NH_3)^+$, even at the highest ammonia flows, was extremely low, and any subsequent addition might plausibly be undetectable against the noise level. Here, we pursued a proton-bound structure $(C_{60}{\cdot}NH_3{\cdot}NH_3)^+$ and several 'double-handled' isomers $(H_3N{\cdot}C_{60}{\cdot}NH_3)^+$ as possible structures for the secondary adduct. While there are, in principle, 23 distinct structural isomers of the double-handled adduct, due to the limitations of computational resources we elected to study only a subset of five such structures. The structures investigated are the 1, *x* isomers, where the index '*x*' is identified as one of the five numbered C atoms on the Schlegel diagram [39] shown in Fig. 2. Only one of the double-handled structures, namely the 1, 55 isomer, optimized. This structure has an overall bond strength for the interaction between the second ammonia and the fullerene cage of 21.3 kJ mol^{-1}, which is very close to the strength of the primary addition, but the adduct now has a much 'looser' structure than the primary product: rather than featuring a discrete C–N bond of around 1.6 Å, the secondary adduct has a C–N distance for each ammonia of 2.86 Å. This long bond, and the slight Mulliken charge localization on ammonia, are both indicative of a weakly-bound electrostatic complex. The $\theta(NCC_\alpha)$ angle for this 'double-handled' adduct of 101.8° is also very close to that of the underivatized fullerene ion. Optimization of this structure, from an 'initial guess' geometry in which each ammonia was within bonding distance of a fullerene C atom, serves to underline the fragility of the primary adduct's C–N bond: it seems that secondary adduct formation (of this type) requires the collision complex to 'cash in' its deformation energy, to progress from having one ammonia closely (but delicately) held to maintaining a loose attraction for two NH_3 units.

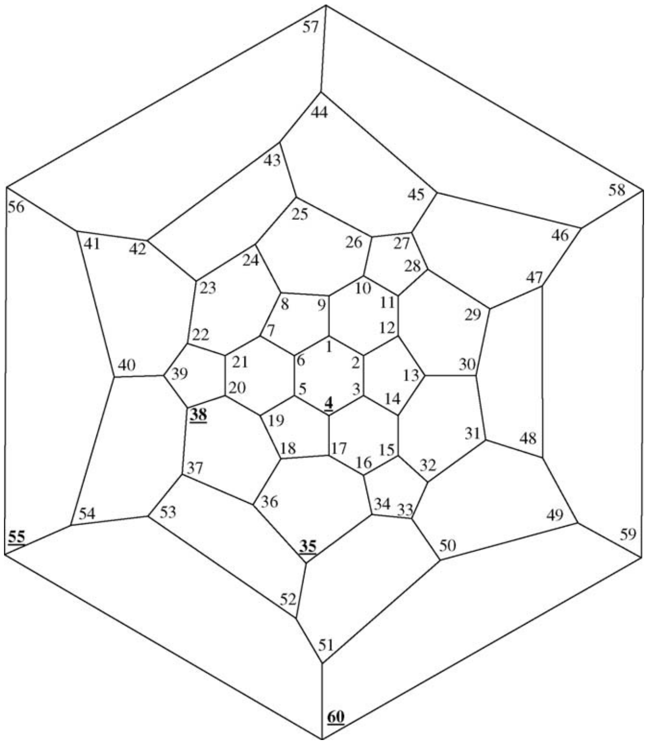

Fig. 2. Schlegel diagram numbering system for the carbon atoms in C_{60} [39].

The other prospective secondary adduct structure to lead to a stationary point, the proton-bound oligomer $(C_{60}{\cdot}NH_3{\cdot}NH_3)^+$, optimized in a straightforward fashion to produce an adduct in which the second ammonia is bound by almost 100 kJ mol^{-1}, i.e., about four times as strongly as the first ammonia. The increase in secondary adduct bond strength, over that of the primary, reflects the influence of local lattice distortion in the first addition step. This secondary adduct possesses a shorter C–N bond (1.56 Å) and a more heavily puckered *ipso* C atom ($\theta(NCC_\alpha) = 110.0°$) than the primary adduct, with also a higher proportion of the original positive charge having moved 'off-planet': the two NH_3 moieties now account for 62% of the total Mulliken charge, up from 52% for the primary adduct. Although the second NH_3 is much more strongly bound from an energetic standpoint, the primary NH_3 retains the lion's share of localized positive charge and is the more 'ammonium-like' of the two ligands: the bridging proton is much closer to this α N atom than to the β N. Formation of this proton-bound secondary adduct is very much more exothermic (by 75 kJ mol^{-1}) than formation of the weakly-bound double-handled electrostatic complex, and is therefore expected to dominate in the production of any secondary adduct. Given the very much greater exothermicity for the second NH_3 addition, it is in fact somewhat surprising that a primary adduct was observed while a secondary was not detected, since considerations of association efficiency (which is generally expected to increase as the exothermicity of association increases) would suggest that the secondary adduct formation should be relatively rapid. It may be that a barrier of some type impedes secondary adduct formation, although this seems inconsistent with the lack of structural deformation required to add the second NH_3. An 'entropic' barrier might nevertheless account for the lack of secondary adduct production. Further experimental investigation of the $C_{60}{}^+/NH_3$ reaction may resolve this apparent dilemma.

Proton transfer from $(C_{60}\cdot NH_3)^+$ to NH_3 competes, in principle, with secondary adduct formation. However, calculations on $C_{60}NH_2$ reveal that this proton transfer process is endothermic by approximately 80 kJ mol^{-1}. This is consistent with the absence of any evidence for proton transfer as a secondary product channel in the experimental study [28] of the reaction between $C_{60}{}^+$ and NH_3—although again, such a channel would be extremely difficult to detect given the very slow primary addition reaction. The endothermicity of proton transfer from $(C_{60}\cdot NH_3)^+$ to NH_3 also tallies with the position of the bridging proton within the optimized geometry of the secondary adduct, as noted above.

3.2. Reaction of NH_3 with $C_{60}{}^{2+}$

Table 2 details the energetic and structural desiderata for the interactions of $C_{60}{}^{2+}$ with NH_3 in a manner entirely analogous to that already described for Table 1 and the monocationic system. The dicationic system is more complicated, both because extensive isomerism is evident among the secondary adducts and because the ground state of the bare fullerene dication is triplet while most of the dicationic adducts have a singlet ground state. Structures for the singlet products are shown in Fig. 3.

The experimental observations [28,29] are that the primary association step is rapid, and that while secondary addition occurs it does so in competition with proton transfer from the dicationic primary adduct to ammonia.

The calculated C–N bond strength in the triplet adduct $(C_{60}\cdot NH_3)^{2+}$ ($^3A''$) is, at 84.6 kJ mol^{-1}, about four times as large as the value for the monocationic adduct. However, in other respects the dicationic and monocationic adducts are remarkably similar, as can be seen by a comparison of their bond lengths, carbon atom pyramidalization, localized N-atom charge, and deformation energy. Intersystem crossing to the singlet surface (which is presumably facile for a species having so many vibrational modes) produces a more strongly bound adduct: interestingly, both the bond strength and the deformation energy of the singlet adduct are approx. 30 kJ mol^{-1} larger than for the triplet adduct. The much higher bond strength for $(C_{60}\cdot NH_3)^{2+}$ (either singlet or triplet) than for $(C_{60}\cdot NH_3)^+$ is in agreement with the experimental observation that the dicationic fullerene ion adds NH_3 very much more rapidly than does the monocation.

Table 2
Energetic and structural details obtained, at the B3-LYP/6-31G** level of theory, for species relevant to the reactions of $C_{60}{}^{2+}$ and secondary ions with ammonia

Species[a]	$E_e(C_{60}X^{n+})$[b] (hartree)	E_{rel}[c] (kJ mol^{-1})	r(C–N) (Å)	$\theta(NCC_\alpha)$[d] (°)	$q_{Mull}(N)$[e]	E_{deform}[f] (kJ mol^{-1})	Other parameters
$C_{60}{}^{2+}$ ($^3A''$) + $2NH_3$	−2285.530568	0.0	–	101.5	–		–
$C_{60}{}^{2+}$ ($^1A'$) + $2NH_3$	−2285.5272257	+8.8	–	101.5	–		–
$(C_{60}\cdot NH_3)^{2+}$ ($^3A''$) + NH_3	−2342.1205753	−84.6	1.591	109.6	+0.58	49.2	
$(C_{60}\cdot NH_3)^{2+}$ ($^1A'$) + NH_3	−2342.1327878	−116.7	1.569	109.9	+0.60	77.9	
$(C_{60}\cdot NH_3\cdot NH_3)^{2+}$ ($^3A''$)	−2398.7236414	−203.6	1.543	110.7	+0.51(α); +0.16(β)		$r(N_\alpha–H) = 1.126$; $r(H–N_\beta) = 1.592$
$(C_{60}\cdot NH_3\cdot NH_3)^{2+}$ ($^1A'$)	−2398.7403045	−247.3	1.510	111.6	−0.03(α); +0.83(β)		$r(N_\alpha–H) = 1.616$; $r(H–N_\beta) = 1.121$
$(H_3N\cdot C_{60}\cdot NH_3)^{2+}$ ($^3A'$), **4**	−2398.680998	−91.6	1.637	109.3	+0.52 × 2	79.7	
$(H_3N\cdot C_{60}\cdot NH_3)^{2+}$ ($^3A'$), **35**	−2398.6987645	−138.3	1.604	109.4	+0.56 × 2	65.8	
$(H_3N\cdot C_{60}\cdot NH_3)^{2+}$ ($^3A'$), **38**	−2398.7001636	−141.9	1.598	109.5	+0.56 × 2	65.2	
$(H_3N\cdot C_{60}\cdot NH_3)^{2+}$ ($^3A'$), **55**	−2398.6993769	−139.9	1.601	109.4	+0.56 × 2	67.6	
$(H_3N\cdot C_{60}\cdot NH_3)^{2+}$ ($^3A'$), **60**	−2398.6988774	−138.6	1.592	109.3	+0.57 × 2	65.8	
$(H_3N\cdot C_{60}\cdot NH_3)^{2+}$ ($^1A'$), **4**	−2398.7178058	−188.3	1.588	109.8	+0.56 × 2	74.9	
$(H_3N\cdot C_{60}\cdot NH_3)^{2+}$ ($^1A'$), **35**	−2398.7150579	−181.0	1.585	109.6	+0.57 × 2	76.2	
$(H_3N\cdot C_{60}\cdot NH_3)^{2+}$ ($^1A'$), **38**	−2398.7007807	−143.6	1.601	109.6	+0.56 × 2	70.6	
$(H_3N\cdot C_{60}\cdot NH_3)^{2+}$ ($^1A'$), **55**	−2398.7084723	−163.7	1.593	109.6	+0.57 × 2	69.4	
$(H_3N\cdot C_{60}\cdot NH_3)^{2+}$ ($^1A'$), **60**	−2398.6979016	−136.0	1.623	109.5	+0.54 × 2	76.9	
$(C_{60}NH_2)^+$ ($^3A''$) + $NH_4{}^+$	−2341.8400746	−262.1	1.470	112.4	−0.01		
$(C_{60}NH_2)^+$ ($^1A'$) + $NH_4{}^+$	−2341.8661496	−330.6	1.475	112.1	+0.01		

[a] For double-handled adducts, the identity of the second anchorage carbon (see Fig. 2) is shown in bold.

[b] Total energy for the identified fullerene-containing species, excluding zero-point vibrational energy.

[c] Energy of the indicated combination of species (at 0 K), expressed relative to the total energy of the three reactants $C_{60}{}^{2+}$ ($^3A''$) + $2NH_3$.

[d] Pyramidalization angle of the anchorage carbon atom(s), defined as detailed in the text.

[e] Calculated Mulliken charge on the nitrogen atom(s), with contributions from H atoms incorporated into N.

[f] Energy of deformation of the anchorage carbon atom, defined as detailed in the text.

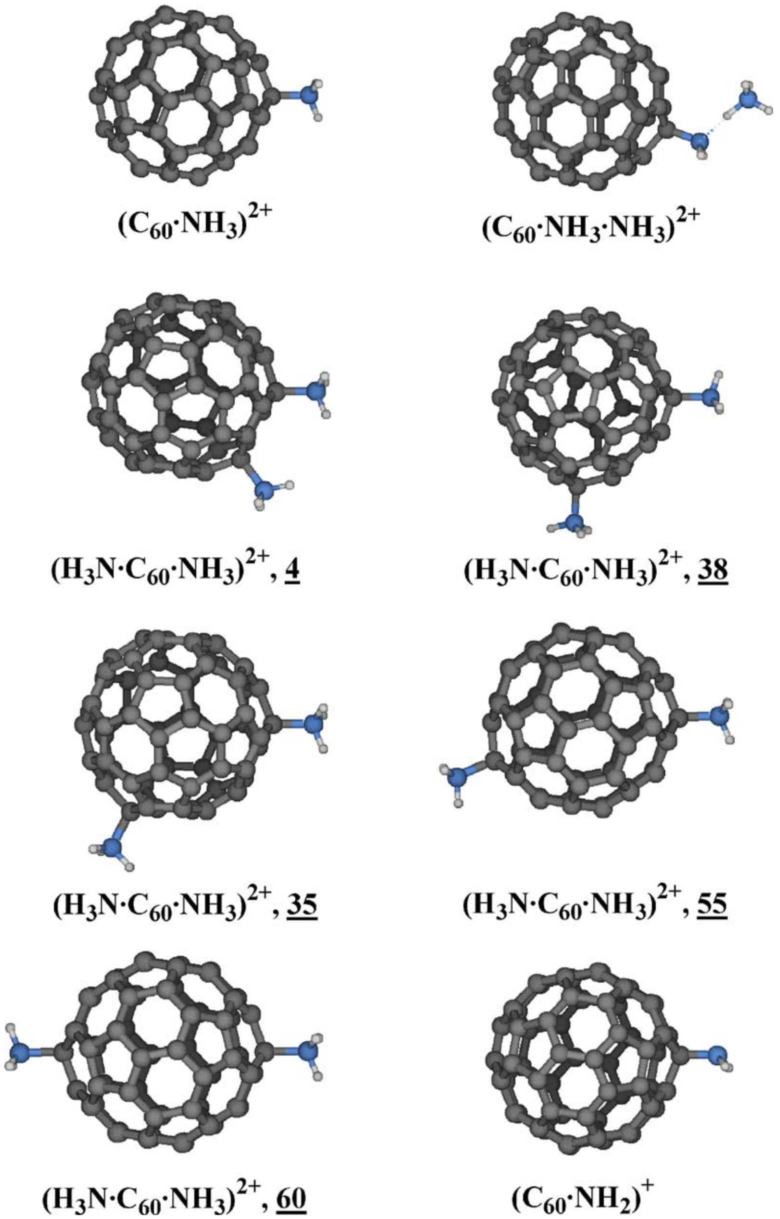

$(C_{60}\cdot NH_3)^{2+}$

$(C_{60}\cdot NH_3\cdot NH_3)^{2+}$

$(H_3N\cdot C_{60}\cdot NH_3)^{2+}$, $\underline{\mathbf{4}}$

$(H_3N\cdot C_{60}\cdot NH_3)^{2+}$, $\underline{\mathbf{38}}$

$(H_3N\cdot C_{60}\cdot NH_3)^{2+}$, $\underline{\mathbf{35}}$

$(H_3N\cdot C_{60}\cdot NH_3)^{2+}$, $\underline{\mathbf{55}}$

$(H_3N\cdot C_{60}\cdot NH_3)^{2+}$, $\underline{\mathbf{60}}$

$(C_{60}\cdot NH_2)^{+}$

Fig. 3. Structures relevant to the reactions of $C_{60}{}^{2+}$ with ammonia. Species shown are singlet-state primary and secondary products optimized at the B3-LYP/6-31G** level of theory. The ‘double-handled’ adducts are identified by the atom number of the second anchorage carbon (see text, and Fig. 2). Optimized geometries of the triplet-state products (which generally lie higher in energy than their singlet-state counterparts) are very similar to those shown here. Similarly, the structures of tricationic adducts explored herein also conform quite closely to the geometries shown here.

There are many structures possible for the secondary adduct $(C_{60}\cdot(NH_3)_2)^{2+}$. Due to computational limitations, we have here investigated (both singlet and triplet electronic states of) only six structures: a proton-bound species, and the five ‘double-handled’ 1, x adducts where atom x is one of those identified in the Schlegel diagram (Fig. 2). The proton-bound structure (‘PB’) appears energetically preferred on either electronic state surface: formation of triplet PB from the triplet primary adduct is approximately 120 kJ mol^{-1} exothermic, while formation of singlet PB from the singlet monoadduct is about 130 kJ mol^{-1} exothermic. There is a significant structural difference between the two electronic states of the proton-bound structure: in the triplet the proton ‘belongs’ to the α N atom, while in the singlet the structure and Mulliken charge distribution is much more in keeping with β N protonation. The singlet PB structure is, in essence, that of a weakly-bound ammonium coordinated to $C_{60}NH_2{}^+$. In fact, the ‘bond strength’ between $C_{60}NH_2{}^+$ and $NH_4{}^+$ is negative, so that dissociation of singlet PB is exothermic: nevertheless, in accordance with other studies on charge separation processes involving fullerene ions [24–26,40], it is expected that a significant Coulombic barrier exists to inhibit fragmentation. Similar considerations apply to triplet PB, whose dissociation is not so severely exothermic and for which the Coulombic barrier is likely larger due to the necessity, during fragmentation, for more complete ‘intra-complex’ proton transfer from the α to the β N.

Since the PB structure is energetically the lowest-lying dicationic adduct of either spin state, it is likely to dominate the secondary adduct composition. However, formation of some double-handled secondary adducts should not be discounted, since these are expected to be local minima, albeit disadvantaged by the repeated imposition of a deformation energy 'toll' for attachment of the second handle. The various double-handled adducts are identified, in Table 2 and in the discussion below, by the site *x* of attachment for the second NH_3. Addition of a second ammonia handle ranges in exothermicity from under 10 kJ mol^{-1} (for formation, from the triplet monoadduct, of triplet **4**) to over 70 kJ mol^{-1} (for spin-conserved formation of singlet **4**). It is particularly interesting to note that structure **4** is, among the singlet-state species surveyed here, the lowest-energy double-handled structure, while also being the highest energy of the triplet-state species. The ordering of stability among the singlet double-handled adducts is quite contrary to the predicted ordering from our phenomenological discussion of double-handled adduct formation [41], in which it was argued that electrostatic considerations would dominate, dictating that an adduct bearing two positively-charged handles would enjoy the greatest stability if these handles were as widely separated as possible (i.e., diametrically opposite each other, at the two 'poles' of the fullerene cage). If this simple electrostatic argument [41] were indeed valid, the stability ordering (from most to least stable) would therefore be **60**, **55**, **35**, **38**, **4**. However, the observed ordering (among singlets) is almost the opposite: **4**, **35**, **55**, **38**, **60**. It appears that this ordering instead reflects the dominant role of fullerene resonance stabilization. A study of such resonance stabilization in the simplest difunctionalized fullerene system, singlet $C_{60}H_2$ [42], has established an approximate relative energy ranking of the 23 feasible doubly-exohedral isomers of $C_{60}H_2$. When the sites of derivatization in our five doubly-handled isomeric singlet dications are compared with the $C_{60}H_2$ results [42], it transpires that the stability ordering of these five isomers agrees perfectly.

Resonance seems to have a smaller (or less readily discernible) impact on the triplet-state double-handled adducts, with **4** exhibiting substantial destabilization relative to the other four (closely clustered) isomers. The C–N distance in **4**, of 1.637 Å, is by a small extent the longest fullerene-nitrogen bond seen in any of the dicationic adducts, while the Mulliken charge per ammonia is also slightly the lowest of any of the double-handled isomers. These observations, in tandem with the comparatively high total energy value for this structure, suggest that triplet **4** is destabilized relative to the other double-handled triplets by the electrostatic crowding of the two ammonias, although the trend in energies for the other triplet isomers does not provide any additional support for this hypothesis.

However, regardless of the electronic state, proton transfer from $(C_{60}\cdot NH_3)^{2+}$ to ammonia is more exothermic than secondary adduct formation. If both reactants and products remain on a triplet surface, proton transfer from $(C_{60}\cdot NH_3)^{2+}$ to NH_3 is almost 180 kJ mol^{-1} exothermic, i.e., about 60 kJ mol^{-1} more exothermic than formation of the triplet-state 'PB' isomer. (The existence of this isomer as a discrete stationary point nevertheless strongly suggests, in keeping with the general picture of charge-separating reactions in the gas-phase, that proton transfer is inhibited by a Coulombic barrier which may well protrude above the energy of reactants.) If reaction between $(C_{60}\cdot NH_3)^{2+}$ and NH_3 occurs on a singlet surface, proton transfer is over 210 kJ mol^{-1} exothermic, i.e., over 80 kJ mol^{-1} more exothermic than formation of the lowest-energy ('PB') singlet isomer of the secondary adduct.

3.3. Reaction of NH_3 with C_{60}^{3+}

The experimental record for the tricationic system [28] is that C_{60}^{3+} reacts with NH_3 solely by addition, despite the ostensible accessibility of charge transfer (on which we comment further below). The primary adduct undergoes further rapid reaction, dominated by proton transfer but with formation of a secondary adduct evident as a minor product channel (with an apparent branching ratio of ∼8:2). Both the proton transfer and addition products also undergo further proton transfer and addition (or at least, the three distinct product formulae – $C_{60}NH^+$, $C_{60}N_2H_5^{2+}$, and $C_{60}N_3H_9^{3+}$ – formed by these four possible tertiary reaction processes are all seen [28]). $C_{60}(NH_3)_3^{3+}$ itself appears to be comparatively unreactive [28].

Before analysing the results of the present calculations (see Table 3) and their implications for the interpretation of the experimental results, it is pertinent to review the absence of charge transfer from C_{60}^{3+} to NH_3 [28] despite the exothermicity of this reaction exceeding, by about 1 eV, the modelled threshold for charge transfer from C_{60}^{3+} to a gas-phase neutral X [25,26]. The model [26] assumes that the charge transfer process occurs at a close interaction of C_{60}^{3+} and X, with the transferred charge initially localized on the 'closest' atom within X and with the fullerene's two residual charges optimally placed (in terms of electrostatic factors) on the fullerene's 'backside'. A rather different picture of the charge-separation process has recently emerged in the context of proton transfer from $C_{60}H^{2+}$ to various neutrals X. Hybrid density functional theory calculations on the proton transfer process, by Harvey and Bathelt [43], have shown that in the transition state to proton transfer the fullerene's residual charge centre is only moderately displaced from the C_{60} centre-of-mass; the nascent charge on XH^+ is generally distributed along the heavy-atom backbone, i.e., with the charge on X significantly further from the fullerene than has been assumed in the early models of fullerene charge separation. However, it seems that for neutrals X with several heavy atoms the errors in the modelled positions of the 'fullerene-charge' and the 'X-charge' largely cancel: Harvey and Bathelt [43] find a separation of charge centres, at the transition state to proton transfer, which is broadly consistent with the modelled charge separation at the transition state, despite the displacement of each charge. For the reaction of C_{60}^{3+} with NH_3, it may well be that the small size of the ammonia molecule results in a higher than generally modelled [25,26] barrier to charge transfer.

As with C_{60}^{2+}, two low-lying electronic states of C_{60}^{3+} are evident in our calculations. Of these, the quartet spin state is marginally the lower energy, but it is consistently the doublet-state adducts which are lower lying. Thus it is likely that intersystem crossing generally operates to effect conversion of quartet-state reactants to doublet-state products.

Formation of the mono-adduct is exothermic by over 140 kJ mol^{-1} for either spin state. Compared to the analogous dicationic primary adduct, the C–N bond in the tricationic adduct is marginally shorter, the pyramidalization angle $\theta(\mathrm{NCC}_\alpha)$ is slightly larger (indicating a small increase in the degree of fullerene 'puckering') and the Mulliken charge on ammonia is somewhat larger. The E_{deform} value is also considerably larger than for the dicationic case.

As with the dicationic system, we have obtained structural and energetic data for a proton-bound secondary adduct and the five double-handled adducts identified with reference to Fig. 2. Again, secondary adduct formation is most exothermic for production of the proton-bound adduct structure (which, for both spin states, has the bridging proton much more tightly bound to the β than to the α nitrogen atom). For the double-handled secondary adducts, the quartet spin state results bear very close resemblance to the triplet dicationic system, with structure **4** again disfavored in an energetic sense relative to the near-isoenergetic set of structures **35**, **38**, **55**, and **60**. There is slightly more definition in the energetic ordering of doublet double-handled adducts, which from lowest to highest energy are **35**, **55**, (**4**, **38**), **60**. As with the dicationic double-handled adducts, charge separation does not appear to be a controlling factor in adduct stability. However, the case for resonance stabilization as an influence is less easily made in the tricationic system, since neither spin state matches the (singlet) model system of $C_{60}H_2$.

Proton transfer from $(C_{60}{\cdot}NH_3)^{3+}$ to NH_3 is dramatically more exothermic than association (by almost 300 kJ mol^{-1}), but as with the dicationic case it is important to remember that this is with reference to product ions *at infinite separation* and there will perforce be severe Coulombic factors leading to barriers to charge separation. This can be seen, in a sense, by noting that even though the dissociation of the proton-bridged doublet secondary adduct $(C_{60}{\cdot}NH_3{\cdot}NH_3)^{3+}$ ($^2A''$) is 287 kJ mol^{-1} exothermic, the bridging proton succeeds in holding the structure together within this stationary point.

Tertiary adduct formation is also evident in the experimental study of the reaction between $C_{60}{}^{3+}$ and NH_3. However, in view of the plethora of possible adduct structures (and the consequent enormity of the computational task) we have elected not to pursue calculations on tertiary adducts in the present work.

3.4. Reaction of NH_3 with $C_{60}NH_2{}^{n+}$ ($n = 1, 2$)

Proton transfer from both $(C_{60}{\cdot}NH_3)^{2+}$ and $(C_{60}{\cdot}NH_3)^{3+}$ to NH_3 is highly exothermic, and both of these primary adducts are seen [28,29] to undergo efficient proton transfer to ammonia at room temperature under the operating conditions of the York SIFT. The proton transfer product ions $C_{60}NH_2{}^{+}$ and $C_{60}NH_2{}^{2+}$ may well undergo further addition with NH_3 to yield respectively, $(C_{60}{\cdot}N_2H_5)^{+}$ and $(C_{60}{\cdot}N_2H_5)^{2+}$, which are both seen as subsequent product ions in the experiments. Alternatively (or concurrently), the latter species may also arise via proton transfer to NH_3 from the secondary adducts $(C_{60}{\cdot}(NH_3))_2{}^{2+}$ and

Table 3
Energetic and structural details obtained, at the B3-LYP/6-31G** level of theory, for species relevant to the reactions of $C_{60}{}^{3+}$ and secondary ions with ammonia

Species[a]	$E_e(C_{60}X^{n+})$[b] (hartree)	E_{rel}[c] (kJ mol^{-1})	r(C–N) (Å)	$\theta(\mathrm{NCC}_\alpha)$[d] (°)	q_{Mull}(N)[e]	E_{deform}[f] (kJ mol^{-1})	Other parameters
$C_{60}{}^{3+}$ ($^4A''$) + $2NH_3$	−2285.0314858	0.0	–	101.5	–		–
$C_{60}{}^{3+}$ ($^2A''$) + $2NH_3$	−2285.0288844	6.8	–	101.5	–		–
$(C_{60}{\cdot}NH_3)^{3+}$ ($^4A''$) + NH_3	−2341.64441	−144.8	1.577	110.5	+0.63	114.6	
$(C_{60}{\cdot}NH_3)^{3+}$ ($^2A''$) + NH_3	−2341.6582765	−181.2	1.559	110.5	+0.65	103.7	
$(C_{60}{\cdot}NH_3{\cdot}NH_3)^{3+}$ ($^4A''$)	−2398.2659168	−312.2	1.509	112.4	−0.02 (α), +0.87 (β)		$r(N_\alpha{-}H) = 1.840$; $r(H{-}N_\beta) = 1.074$
$(C_{60}{\cdot}NH_3{\cdot}NH_3)^{3+}$ ($^2A''$)	−2398.2872815	−368.2	1.505	112.2	−0.01 (α), +0.89 (β)		$r(N_\alpha{-}H) = 1.901$; $r(H{-}N_\beta) = 1.066$
$(H_3N{\cdot}C_{60}{\cdot}NH_3)^{3+}$ ($^4A''$), **4**	−2398.227177	−210.4	1.605	110.3	+0.58 × 2	65.0	
$(H_3N{\cdot}C_{60}{\cdot}NH_3)^{3+}$ ($^4A''$), **35**	−2398.2468699	−262.1	1.583	110.2	+0.61 × 2	67.3	
$(H_3N{\cdot}C_{60}{\cdot}NH_3)^{3+}$ ($^4A''$), **38**	−2398.2470022	−262.5	1.582	110.3	+0.61 × 2	66.6	
$(H_3N{\cdot}C_{60}{\cdot}NH_3)^{3+}$ ($^4A''$), **55**	−2398.2476708	−264.3	1.582	110.1	+0.61 × 2	68.4	
$(H_3N{\cdot}C_{60}{\cdot}NH_3)^{3+}$ ($^4A''$), **60**	−2398.2499552	−270.2	1.577	110.0	+0.62 × 2	74.2	
$(H_3N{\cdot}C_{60}{\cdot}NH_3)^{3+}$ ($^2A''$), **4**	−2398.2669323	−314.8	1.574	110.5	+0.61 × 2	100.6	
$(H_3N{\cdot}C_{60}{\cdot}NH_3)^{3+}$ ($^2A''$), **35**	−2398.2728374	−330.3	1.567	110.3	+0.63 × 2		
$(H_3N{\cdot}C_{60}{\cdot}NH_3)^{3+}$ ($^2A''$), **38**	−2398.2662643	−313.1	1.570	110.3	+0.62 × 2	75.3	
$(H_3N{\cdot}C_{60}{\cdot}NH_3)^{3+}$ ($^2A''$), **55**	−2398.2707425	−324.8	1.568	110.3	+0.63 × 2	76.8	
$(H_3N{\cdot}C_{60}{\cdot}NH_3)^{3+}$ ($^2A''$), **60**	−2398.2615123	−300.6	1.571	110.1	+0.63 × 2	78.6	
$(C_{60}NH_2)^{2+}$ ($^4A''$) + $NH_4{}^{+}$	−2341.4647943	−587.2	1.460	112.7	+0.05		
$(C_{60}NH_2)^{2+}$ ($^2A''$) + $NH_4{}^{+}$	−2341.4908843	−655.7	1.465	112.3	+0.07		

[a] For double-handled adducts, the identity of the second anchorage carbon (see Fig. 2) is shown in bold.

[b] Total energy for the identified fullerene-containing species, excluding zero-point vibrational energy.

[c] Energy of the indicated combination of species (at 0 K), expressed relative to the total energy of the three reactants $C_{60}{}^{2+}$ ($^3A''$) + $2NH_3$.

[d] Pyramidalization angle of the anchorage carbon atom(s), defined as detailed in the text.

[e] Calculated Mulliken charge on the nitrogen atom(s), with contributions from H atoms incorporated into N.

[f] Energy of deformation of the anchorage carbon atom, defined as detailed in the text.

Table 4
Energetic details obtained, at the B3-LYP/6-31G** level of theory, for species relevant to the proton-transfer chemistry initiated by dicationic and tricationic reactant fullerene ions

Species[a]	$E_e(C_{60}X^{n+})$[b] (hartree)	ΔE_{react}(AAP)[c] (kJ mol^{-1})	ΔE_{react}(APA)[c] (kJ mol^{-1})	ΔE_{react}(ABS)[c] (kJ mol^{-1})	ΔE_{react}(APP)[c] (kJ mol^{-1})
$(H_3N\cdot C_{60}\cdot NH_2)^{1+}$ (^1A), **4**	−2398.4487461	−116.7/−71.6/−207.5	−116.7/−213.9/−65.2	−116.7/−130.6/−148.5	–
$(H_3N\cdot C_{60}\cdot NH_2)^{1+}$ (^1A), **35**	−2398.4215113	−116.7/−64.3/−143.2	−116.7/−213.9/+6.3	−116.7/−130.6/−76.9	–
$(H_3N\cdot C_{60}\cdot NH_2)^{1+}$ (^1A), **55**	−2398.4145082	−116.7/−47.0/−142.1	−116.7/−213.9/+24.7	−116.7/−130.6/−58.5	–
$C_{60}NH$ ($^1A'$)	−2341.385063	–	–	–	−116.7/−213.9/+349.2
$(H_3N\cdot C_{60}\cdot NH_2)^{2+}$ ($^2A'$), **4**	−2398.0967324	−181.2/−133.6/−467.1	−181.2/−474.5/−126.2	−181.2/−187.0/−413.7	–
$(H_3N\cdot C_{60}\cdot NH_2)^{2+}$ (^2A), **35**	−2398.0810136	−181.2/−149.1/−410.3	−181.2/−474.5/−85.0	−181.2/−187.0/−372.4	–
$(H_3N\cdot C_{60}\cdot NH_2)^{2+}$ (^2A), **38**	−2398.0774196	−181.2/−131.9/−418.1	−181.2/−474.5/−75.5	−181.2/−187.0/−363.0	–
$(H_3N\cdot C_{60}\cdot NH_2)^{2+}$ (^2A), **55**	−2398.0798474	−181.2/−143.6/−412.7	−181.2/−474.5/−81.9	−181.2/−187.0/−369.3	–
$(H_3N\cdot C_{60}\cdot NH_2)^{2+}$ ($^2A'$), **60**	−2398.0738503	−181.2/−119.4/−421.7	−181.2/−474.5/−66.2	−181.2/−187.0/−354.1	–
$C_{60}NH^+$ ($^2A''$)	−2341.1944347	–	–	–	−181.2/−474.5/−135.6

[a] For double-handled adducts, the identity of the second anchorage carbon (see Fig. 2) is shown in bold.

[b] Total energy for the identified fullerene-containing species, excluding zero-point vibrational energy.

[c] Energy of reaction (at 0 K) for each of the three sequential steps involved in the identified proton-transfer scheme (see text for details). A negative value indicates an energy-releasing (exoergic) step.

$(C_{60}\cdot(NH_3))_2{}^{3+}$. We have therefore obtained structural and energetic data for several species of the formula $(C_{60}\cdot N_2H_5)^{n+}$, to attempt to ascertain by which mechanism(s) these species are formed. The total energies and reaction energies for these species are shown in Table 4, while the optimized geometries of species relevant to the chemistry initiated by $C_{60}{}^{3+} + NH_3$ are shown in Fig. 4.

From the starting point of $C_{60}{}^{2+} + NH_3$, we have isolated four prospective tertiary products: isomers **4**, **35**, and **55** of the structural formula $(H_3N\cdot C_{60}\cdot NH_2)^{1+}$ (^1A) (where the number again refers to the site of second derivatization, as in Fig. 2), and $C_{60}NH$. A bridged structure $(C_{60}\cdot N_2H_5)^{1+}$ was also investigated, but did not lead to an intact stationary point. (We have explored only the singlet spin state for each structure, since it is probable that intersystem crossing to the energetically preferred singlet-state occurs readily during the primary addition step.) As noted above, the double-handled species can arise in more than one way. One sequence, which we label 'AAP' (i.e., add, add, proton transfer), is

$$C_{60}{}^{2+} + NH_3 + M \rightarrow (C_{60}\cdot NH_3)^{2+} + M^* \tag{3}$$

$$(C_{60}\cdot NH_3)^{2+} + NH_3 + M \rightarrow (H_3N\cdot C_{60}\cdot NH_3)^{2+} + M^* \tag{4}$$

$$(H_3N\cdot C_{60}\cdot NH_3)^{2+} + NH_3 \rightarrow (H_3N\cdot C_{60}\cdot NH_2)^{+} + NH_4{}^{+} \tag{5}$$

a second sequence,

$$C_{60}{}^{2+} + NH_3 + M \rightarrow (C_{60}\cdot NH_3)^{2+} + M^*$$

$$(C_{60}\cdot NH_3)^{2+} + NH_3 \rightarrow (C_{60}\cdot NH_2)^{+} + NH_4{}^{+} \tag{6}$$

$$(C_{60}\cdot NH_2)^{+} + NH_3 + M \rightarrow (H_3N\cdot C_{60}\cdot NH_2)^{+} + M^* \tag{7}$$

may be abbreviated as 'APA' (add, proton transfer, add), while a third possibility,

$$C_{60}{}^{2+} + NH_3 + M \rightarrow (C_{60}\cdot NH_3)^{2+} + M^*$$

$$(C_{60}\cdot NH_3)^{2+} + NH_3 + M \rightarrow (C_{60}\cdot NH_2\cdot NH_4)^{2+} + M^* \tag{8}$$

$$(C_{60}\cdot NH_2\cdot NH_4)^{2+} + NH_3 \rightarrow (H_3N\cdot C_{60}\cdot NH_2)^{+} + NH_4{}^{+} \tag{9}$$

may be termed 'ABS' (add, bridge, switch). The AAP and ABS mechanisms are exothermic for all three steps, for each of the optimized $(H_2N\cdot C_{60}\cdot NH_3)^{1+}$ isomers, but the APA mechanism is consistently exothermic only for production of $(H_2N\cdot C_{60}\cdot NH_3)^{1+}$ isomer **4**, with the final addition step found to be mildly endothermic for **35** and more strongly endothermic for **55**. Clearly, however, any mechanism favours production of $(H_2N\cdot C_{60}\cdot NH_3)^{1+}$ isomer **4**, as the lowest-energy ion of this formula (among the limited set of structures explored in the present work). The ABS mechanism is advantaged in the sense that it involves the lowest-energy secondary adduct, whereas the AAP mechanism requires the formation of a higher-energy secondary adduct; however, the greater exothermicity of the final charge-separating step in AAP means that this step is arguably more likely to overcome the Coulombic barrier to charge separation, while ABS may fail in this regard.For the sake of curiosity, we have also investigated the possibility of an 'APP' (add, proton transfer, proton transfer) reaction sequence:

$$C_{60}{}^{2+} + NH_3 + M \rightarrow (C_{60}\cdot NH_3)^{2+} + M^*$$

$$(C_{60}\cdot NH_3)^{2+} + NH_3 \rightarrow (C_{60}\cdot NH_2)^{+} + NH_4{}^{+}$$

$$(C_{60}\cdot NH_2)^{+} + NH_3 \rightarrow C_{60}\cdot NH + NH_4{}^{+} \tag{10}$$

however, the final step (10) is severely endothermic and thus this reaction (to which the SIFT would be essentially blind, since $C_{60}\cdot NH$ is undetectable and $NH_4{}^+$ is produced in earlier steps) cannot occur.

A similar extrapolation can be performed for the products of $C_{60}{}^{3+} + NH_3$. Here again we assume that intersystem crossing is facile and occurs on the primary addition step. Thereafter each

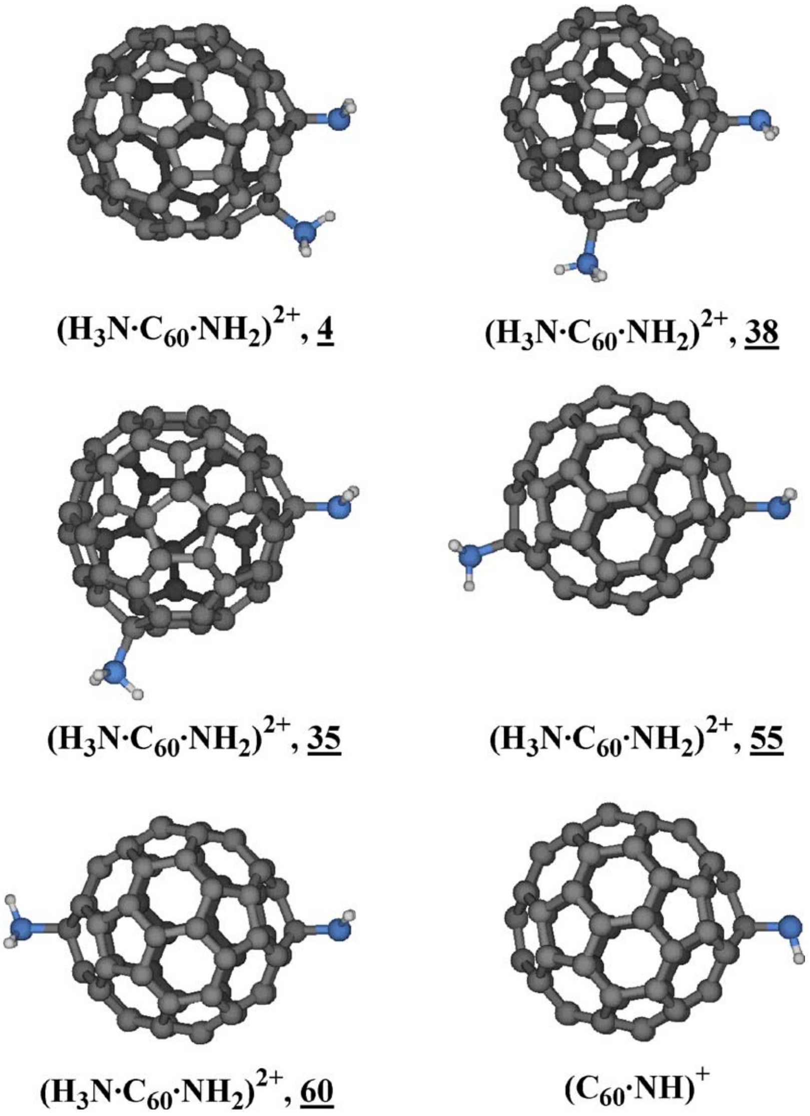

$(H_3N{\cdot}C_{60}{\cdot}NH_2)^{2+}$, **4**

$(H_3N{\cdot}C_{60}{\cdot}NH_2)^{2+}$, **38**

$(H_3N{\cdot}C_{60}{\cdot}NH_2)^{2+}$, **35**

$(H_3N{\cdot}C_{60}{\cdot}NH_2)^{2+}$, **55**

$(H_3N{\cdot}C_{60}{\cdot}NH_2)^{2+}$, **60**

$(C_{60}{\cdot}NH)^{+}$

Fig. 4. Structures relevant to the reactions of doublet $C_{60}NH_2^{2+}$ (formed as a secondary product from $C_{60}^{3+} + NH_3$) with ammonia. The 'double-handled' adducts are identified by the atom number of the second anchorage carbon (see text, and Fig. 2).

of the AAP, APA, and ABS mechanisms is consistently exothermic throughout, regardless of which of the $(H_3N{\cdot}C_{60}{\cdot}NH_2)^{2+}$ isomers is considered. (Again, a bridged structure $(C_{60}{\cdot}N_2H_5)^{2+}$ was considered, but was not stable.) Exothermic also is the APP channel, in keeping with the observation of the species $C_{60}NH^+$ as a product in this system, although the comparatively low exothermicity of the final proton transfer step may be insufficient to surmount the Coulombic barrier to charge separation. It may well be that this product channel occurs via proton transfer from 'hot' $C_{60}NH_2^{2+}$, since the latter ion is produced by a highly exothermic charge-separation step.

Deprotonation of $(C_{60}{\cdot}NH_3)^{3+}$ to give $(C_{60}{\cdot}NH_2)^{2+}$ results in a contraction of the C–N distance, from 1.577 to 1.465 Å, and an increase in the pyramidalization parameter $\theta(NCC_\alpha)$ from 110.5° to 112.3°. Further deprotonation to give $(C_{60}{\cdot}NH)^+$ has much less structural impact, with the C–N distance at 1.465 Å and $\theta(NCC_\alpha)$ at 112.0°. These values are also very close to those for $(C_{60}{\cdot}NH_2)^+$. So far as we can establish, none of these species (for which the nitrogen atom is formally valence-unsatisfied) show any inclination to adopt a bridged structure (such as proposed in the original experimental studies [28,29]) in which the N is bonded to two adjacent C atoms. One reason for why such a structure might be disfavored is the extreme puckering which would be required: if pyramidalization of one carbon is associated with an E_{deform} value of 50–120 kJ mol^{-1}, then the pyramidalization of two adjacent carbons (to form, moreover, a three-membered ring) is very likely to be prohibitive.

3.5. General discussion

The present work should be viewed merely as a preliminary investigation of the reactions of fullerene ions with ammonia. Due to the computational expense of the calculations involved, we have not pursued vibrational frequency calculations on the species studied. We have not explored any of the (many) feasible tertiary adduct structures, and have restricted our studies here to only a subset of the possible secondary adduct structures. Because of these limitations, the results reported here cannot properly be regarded as definitive. Nonetheless, there are many aspects of the present work which add to our picture of fullerene reactivity. First, it is gratifying that the theoretical results appear largely supportive of the experimental record for the fullerene ion/ammonia reactions [28,29]. Second, it is obvious that addition to a fullerene ion is not without cost, from the perspective of the carbon cage: puckering of the fullerene framework surrounding the anchorage carbon atom requires 50 kJ mol^{-1} or more in strain energy, which must be supplied by the interaction between the fullerene ion and the reactant neutral if association is to succeed. Third, it is notable that the stability of the doubly-charged double-handled adducts (and, though less obviously, their tricationic analogues) does not conform to the simple electrostatic model which was developed from the original experimental studies. Rather, there is an important and apparently dominant resonance stabilization contribution to the relative energies of the various double-handled isomers. Fourth, while there is clearly competition between exothermic proton transfer and secondary addition in the reactions initiated by C_{60}^{2+} and C_{60}^{3+} with NH_3, it is not possible to discern which of several mechanisms is principally responsible for the formation of the species $(H_3N{\cdot}C_{60}{\cdot}NH_2)^{n+}$ ($n = 1, 2$).

Quantification of the fullerene deformation energy for *exo* bond formation allows us to extrapolate, in some sense, to larger systems. For larger highly symmetric fullerenes, the surface at any C atom is more nearly planar and thus a greater degree of puckering (with, presumably, a larger E_{distort} value) will be required for derivatization of the fullerene cage. This suggests that larger symmetric fullerene ions may be more selective in their association chemistry. Similar considerations apply also to carbon nanotubes (excepting the tube ends). However, less symmetric fullerenes such as C_{70} may feature some C atoms for which pyramidalization is not such a strain, and it is these sites at which association is likely to be preferred. For this reason, a theoretical investigation of the association propensities of C_{70}^{+} with ammonia (for which experimental kinetic data already exist [28,29]) would be of considerable interest.

4. Conclusions

Fullerene ions in the charge states C_{60}^{+}, C_{60}^{2+} and C_{60}^{3+} are all found to add at least two NH_3 molecules, in broad agreement with experiment. The energetic cost of deformation of the fullerene framework, required for *exo* bond formation to a fullerene C atom, almost negates the intrinsic strength of the C_{60}^{+}–NH_3 bond, accounting for the extreme inefficiency of the monocationic association process to ammonia. By analogy, it appears likely that weaker bases (electron-pair donors) will generally be incapable of overcoming the deformation energy, consistent with the unreactivity of C_{60}^{+} to most simple organic and inorganic molecules.

Acknowledgements

This work made extensive use of the supercomputing resources of the Australian Partnership of Advanced Computing, housed at the ANU Supercomputer Facility. The author thanks Jeremy Harvey for providing access to work in press.

References

[1] A. Hirsch, Chemistry of the Fullerenes, Thieme, Stuttgart, Germany, 1994.
[2] A.B. Smith III (Ed.), Fullerene Chemistry, Pergamon, Oxford, UK, 1996.
[3] A. Hirsch (Ed.), Fullerenes and Related Structures, Springer, Berlin, Germany, 1999.
[4] R. Taylor, Lecture Notes on Fullerene Chemistry: A Handbook for Chemists, Imperial College Press, London, UK, 1999.
[5] W. Andreoni (Ed.), The Physics of Fullerene-Based and Fullerene-Related Materials, Kluwer, Dordrecht, The Netherlands, 2000.
[6] K.M. Kadish, R.S. Ruoff (Eds.), Fullerenes: Chemistry, Physics, and Technology, Wiley, New York, NY, 2000.
[7] P.V. Kamat, D.M. Guldi, K.M. Kadish (Eds.), Fullerenes 2000—Volume 10: Chemistry and Physics of Fullerenes and Carbon Nanomaterials, Electrochemical Society, Pennington, NJ, 2000.
[8] M. Prato (Ed.), Functionalised Fullerene Materials, Royal Society of Chemistry, Cambridge, UK, 2002.
[9] H.W. Kroto, J.R. Heath, S.C. O'Brien, R.F. Curl, R.E. Smalley, Nature 318 (1985) 162.
[10] W. Krätschmer, L.D. Lamb, K. Fostiropoulos, D.R. Huffmann, Nature 347 (1990) 354.
[11] P. Scheier, B. Dünser, R. Wörgötter, S. Matt, D. Muigg, G. Senn, T.D. Märk, Int. Rev. Phys. Chem. 15 (1996) 93.
[12] S. Diaz-Tendero, M. Alcami, F. Martin, Phys. Rev. Lett. 95 (2005) 013401.
[13] J.R. Bowser, Adv. Organomet. Chem. 36 (1994) 57.
[14] C. Bellavia-Lund, J.-C. Hummelen, M. Keshavarz-K, R. Gonzalez, F. Wudl, J. Phys. Chem. Solids 58 (1997) 1983.
[15] H. Schwarz, T. Weiske, D.K. Bohme, J. Hrusak, in: W.E. Billups, M.A. Ciufolini (Eds.), Buckminsterfullerenes, VCH, New York, NY, 1993, p. 257.
[16] H. Shinohara, Rep. Prog. Phys. 63 (2000) 843.
[17] T. Akasaka, S. Nagase (Eds.), Endofullerenes: A New Family of Carbon Clusters, Kluwer, Dordrecht, The Netherlands, 2002.
[18] P. Scheier, B. Dunser, G. Senn, H. Drexel, H.P. Winter, F. Aumayr, G. Betz, F. Biasioli, T. Fiegele, T.D. Märk, Eur. Phys. J. D: Atom. Mol. Opt. Phys. 9 (1999) 91.
[19] D.K. Bohme, Chem. Rev. 92 (1992) 1487.
[20] S. Petrie, D.K. Bohme, Can. J. Chem. 72 (1993) 577.
[21] D.K. Bohme, Int. Rev. Phys. Chem. 13 (1994) 163.
[22] D.K. Bohme, Can. J. Chem. 77 (1999) 1453.
[23] J.A. Zimmerman, J.R. Eyler, S.B.H. Bach, S.W. McElvany, J. Chem. Phys. 94 (1991) 3556.
[24] S. Petrie, G. Javahery, J. Wang, D.K. Bohme, J. Phys. Chem. 96 (1992) 6121.
[25] G. Javahery, H. Wincel, S. Petrie, D.K. Bohme, Chem. Phys. Lett. 204 (1993) 473.
[26] S. Petrie, J. Wang, D.K. Bohme, Chem. Phys. Lett. 204 (1993) 473.
[27] H. Steger, J. de Vries, B. Kamke, W. Kamke, T. Drewello, Chem. Phys. Lett. 194 (1992) 452.
[28] G. Javahery, S. Petrie, H. Wincel, J. Wang, D.K. Bohme, J. Am. Chem. Soc. 115 (1993) 5716.
[29] G. Javahery, S. Petrie, A. Ketvirtis, J. Wang, D.K. Bohme, Int. J. Mass Spectrom. Ion Process. 116 (1992) R7.
[30] J.J. Stry, M.T. Coolbaugh, E. Turos, J.F. Garvey, J. Am. Chem. Soc. 114 (1992) 7914.
[31] A.D. Becke, J. Chem. Phys. 98 (1993) 5648.
[32] C. Lee, W. Yang, R.G. Parr, Phys. Rev. B 37 (1988) 785.

[33] S.F. Boys, F. Bernardi, Mol. Phys. 19 (1970) 553.

[34] M.J. Frisch, G.W. Trucks, H.B. Schegel, G.E. Scuseria, M.A. Robb, J.R. Cheeseman, V.G. Zakrzewski, J.A. Montgomery Jr., R.E. Stratmann, J.C. Burant, S. Dapprich, J.M. Millam, A.D. Daniels, K.N. Kudin, M.C. Strain, O. Farkas, J. Tomasi, V. Barone, M. Cossi, R. Cammi, B. Mennucci, C. Pomelli, C. Adamo, S. Clifford, J.W. Ochterski, G.A. Petersson, P.Y. Ayala, Q. Cui, K. Morokuma, D.K. Malick, A.D. Rabuck, K. Raghavachari, J.B. Foresman, J. Cioslowski, J.V. Ortiz, B.B. Stefanov, G. Liu, A. Liashenko, P. Piskorz, I. Komaromi, R. Gomperts, R.L. Martin, D.J. Fox, T. Keith, M.A. Al-Laham, C.Y. Peng, A. Nanayakkara, C. Gonzalez, M. Challacombe, P.M.W. Gill, B.G. Johnson, W. Chen, M.W. Wong, J.L. Andres, M. Head-Gordon, E.S. Replogle, J.A. Pople, GAUSSIAN98 (Rev. A.7), Gaussian, Inc., Pittsburgh, PA, 1998.

[35] J.A. Montgomery Jr., J.W. Ochterski, G.A. Petersson, J. Chem. Phys. 101 (1994) 5900.

[36] G. Javahery, S. Petrie, J. Wang, H. Wincel, D.K. Bohme, J. Am. Chem. Soc. 115 (1993) 9701.

[37] G. Javahery, S. Petrie, H. Wincel, J. Wang, D.K. Bohme, J. Am. Chem. Soc. 115 (1993) 6295.

[38] S. Petrie, D.K. Bohme, Nature 365 (1993) 426.

[39] R. Taylor, J. Chem. Soc. Perkin Trans. 2 (1993) 813.

[40] S. Petrie, G. Javahery, H. Wincel, D.K. Bohme, J. Am. Chem. Soc. 115 (1993) 6290.

[41] S. Petrie, G. Javahery, D.K. Bohme, J. Am. Chem. Soc. 115 (1993) 1445.

[42] S. Narita, T. Morikawa, T.-I. Shibuya, J. Mol. Struct. (Theochem) 528 (2000) 263.

[43] J.N. Harvey, C. Bathelt, Int. J. Mass Spectrom. 249–250 (2006) 359–363.